

Study of two-electron one-photon transition produced in collision of Ne^{6+} ions with Al target at low energies

Shashank Singh

Department of Physics, Panjab University, Chandigarh-160014, India.

Mumtaz Oswal

Department of Physics, DAV College, Sector 10, Chandigarh-160011, India.

K. P. Singh

Department of Physics, Panjab University, Chandigarh-160014, India.

D. K. Swami

Inter-University Accelerator Centre, Aruna Asaf Ali Marg, Near Vasant Kunj, New Delhi-110067, India.

T. Nandi*

1003 Regal, Mapsko Royal Ville, Sector-82, Gurgaon-122004, India.†

(Dated: January 10, 2022)

Two-electron one-photon transitions have been successfully observed for the Ne projectile and Al target at low energy regime. Experimental energy values of two-electron one-photon transitions are compared with previously reported theoretical and experimental values. Ionization cross-section of two-electron one-photon transition is reported.

I. INTRODUCTION

In the heavy ion-atom collision processes, multiple ionization of different shells created simultaneously is a common phenomenon. For a particular case, K shell of the target or projectile may be doubly ionized during ion-atom collision. Usually, these two vacancies of the K shell is filled by the subsequent electron of the higher shell and as a resultant, characteristics x-rays or Auger electron are emitted. Normally two vacancies are filled in two steps, firstly a hypersatellite line is emitted and secondly a satellite x-ray line as pictorially shown in Fig. 1. Nevertheless, according to Heisenberg [1], Condon [2], and Goudsmit and Gropper [3], it is possible that both the vacancies of the K shell may be filled by a simultaneous transition of two electrons of upper shells. The simultaneous transition of two electrons to fill both K shell vacancies leads emission of one photon of energy of marginally higher than the double of the K shell transition energy. The energy of the two electron one photon (TEOP) transition (also called cooperative transition - $K^{-2} - L^{-2}$) can be estimated as the sum of the transition energies of hypersatellite ($K^{-2} - K^{-1}L^{-1}$) and satellite transition ($K^{-1}L^{-1} - L^{-2}$). In this estimation the vacancy in M or higher shells can be ignored as their effect is very small. The schematic diagram of the TEOP transition is shown in the Fig. 1.

Firstly, Wölfl *et al.* [4] reported two electron one photon transition for Ni-Ni and Ni-Fe systems at beam en-

ergies ≈ 0.8 MeV/amu. Åberg *et al.* [5] showing that the two electron and one photon transition are due to the $1s^{-2} \rightarrow 2s^{-1}2p^{-1}$ electric dipole transition by calculations of Hartee-Fock energy and intensity. Various authors Wölfl and Betz [6], Nagel *et al.* [7], [5] and Knudson *et al.* [8] reported the theoretical prediction of TEOP transition energies in different systems to compare observed energies. In which Hartee-Fock calculations have shown consistent result with the observed transition energies. Stoller *et al.* [9] reported the TEOP transitions for Al-Al, O-Ca, Ca-Ca, Fe-Fe, Fe-Ni, Ni-Fe and Ni-Ni systems at the beam energies between 24 to 40 MeV. In this study, cross-sections of characteristic transitions and TEOP transitions were determined. Also, branching ratios between one and two electron transitions in doubly ionized K shell were determined to compare with various theoretical predictions and found in qualitative agreement. Besides the ion-atom collisions, Auerhammer *et al.* [10] studied the TEOP transition for the Al target with electrons of energy 20 keV using high resolution crystal spectrometer.

Mukherjee *et al.* [11] evaluated the branching ratio between one-electron one photon (OEOP) and TEOP transition in doubly ionized K shell using an equivalent two-particle model with wave functions including angular correlations and relaxation in the length and velocity gauges. Mukherjee and Mukherjee [12] reported the theoretical estimation of excitation energies and transition probabilities for TEOP transition for the inner shell ionised atoms for Ne, Na, Mg, Al, Si, P, S, Cl and Ar. Also, the transition data presented for $K_{\alpha\alpha}^S$ transition ($2s^12p^1 \rightarrow 1s^2$) of the highly stripped He like ions Ne^{8+} , Na^{9+} , Mg^{10+} , Al^{11+} , Si^{12+} , P^{13+} , S^{14+} , Cl^{15+} and Ar^{16+} . Hoszowska *et al.* [13] observed first time TEOP transition in Mg,

* nanditapan@gmail.com

† superannuated from Inter-University Accelerator Centre, Aruna Asaf Ali Marg, Near Vasant Kunj, New Delhi-110067, India.

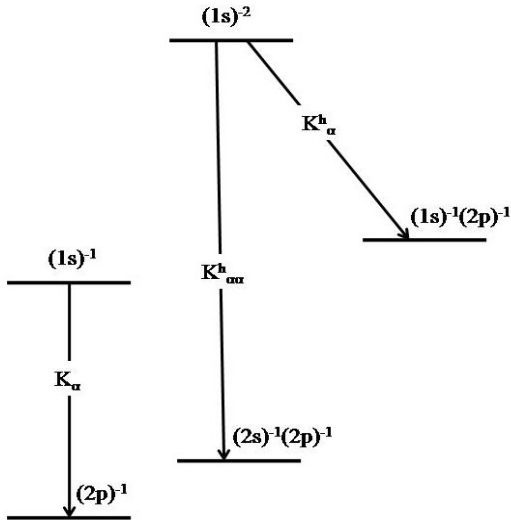


FIG. 1. Schematic diagram of the two electron one photon transition

Al and Si by monochromatized synchrotron radiation using a wavelength dispersive spectrometer. Kasthuri-rangan *et al.* [14] reported first time observation of the fluorescence-active doubly excited states in He-like Si, S and Cl ions. Both the transitions OEOP and TEOP are very sensitive to Breit interaction, quantum electrodynamics (QED), and electron correlations [15–17].

The study of TEOP at low energy heavy ions is very few in literature and study of it is very important for highly stripped ions of He sequence [18, 19] as these ions present in solar corona, flares and laboratory tokamak plasmas. So the less availability of literature at low energy heavy ions and importance of TEOP in various fields makes the TEOP study of high demand.

II. EXPERIMENTAL DETAILS

This experiment was performed at LEIBF facility, IUAC, New Delhi. In this experiment, we took Ne beam of 6+ charge state (1.8 and 2.1 MeV) from ECR ion source placed on a high voltage deck of 400 kV to bombard the Al target. The atomic physics chamber is situated at 75° beam line of LEIBF facility. The schematic diagram of scattering chamber with experimental setup is shown in Fig. 2. High vacuum was maintained inside the chamber using turbo-molecular pump. To measure the x-rays, one silicon drift detector (SDD) was mounted at 90° (detector 1) and another SDD was mounted at 135° (detector 2) with respect to the beam direction. The specification of the detectors (KETEK AXAS-A) are as follows: active area is 20 mm², thickness of Beryllium

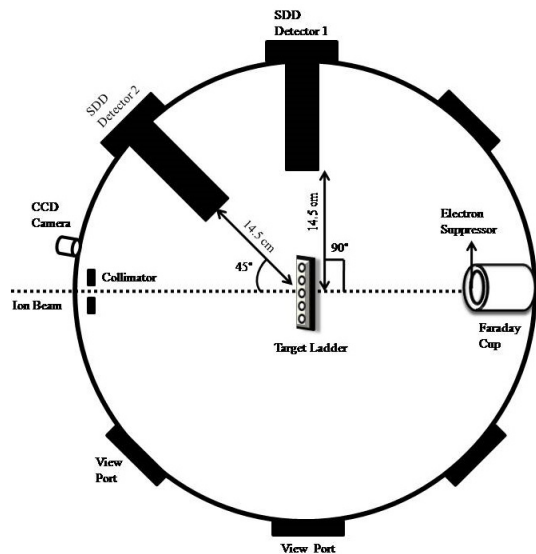


FIG. 2. Schematic diagram of the x-ray spectroscopy setup at LEIBF facility, IUAC, New Delhi

window is 8μm and FWHM is 124.2 eV for Mn K_{α} x-rays. The target ladder was mounted 90° with respect to the beam direction. The target ladder could have five targets at a time and could be vertically displaced by a manual target manipulator. The distance between the target ladder and detectors was 14 cm. To measure the incident charge on target, one Faraday cup was mounted behind the target and attached to the current integrator. A collimator of 5 mm was placed inside the chamber in the line of beam entrance and 18 cm before the target ladder. Thin (thickness = 20μg/cm²) and spectroscopically pure target of Al was mounted on the target ladder. The thickness of the target was measured by energy loss method using α-beam from ²⁴¹Am source.

The thickness of mylar window of chamber for detector 1 and detector 2 were 6μm and 10μm, respectively. The energy calibration was done before and after the experiment using ²⁴¹Am radioactive source. One position of the target of the target ladder was kept empty to take blank run. At another position of the target ladder a quartz crystal was placed to visualize the beam position. The online data was acquired using a CAMAC based software called FREEDOM developed at IUAC [20].

III. RESULTS AND DISCUSSION

K x-ray spectra were recorded for Ne beam on Al-target at 1.8 and 2.1 MeV. Corresponding spectra have been shown in the Fig. 3. Fig. 3(C₁) shows the raw spectrum containing a prominent Bremsstrahlung background. Subtracting the background from the raw spectrum we obtain the real nature of the spectrum. The back

ground subtracted spectrum is shown in Fig. 3(D_1). It shows only a good peak structure around 1.5 keV, which can be fitted into three Gaussian structures as shown with green lines. The same treatment is done on the raw spectrum obtained at 2.1 keV. Here, we seen the similar structure around 1.5 keV along with an additional structure around 3.0 keV. In order to check the ingenuity of the second structure we took a look on raw background spectrum, meaning the beam was passed through the target holder and without the target foil. The raw spectrum display exactly the same shape that we subtracted from the raw spectrum obtained with the target foils. It ensures the fact that the beam hallow hits the target frame. Now, similar back ground subtraction treatment done on the background spectrum displays a structure closed to 3 keV. Thus, such appearance questions on the ingenuity of the structure that pops up with the 2.1 MeV spectrum.

This time instead of subtracting the background shown above, we subtract the actual background from the raw spectrum. This routine certainly deducted the contribution of the actual background from the spectrum and provided us the concrete shape of the spectrum. The correct spectrum so obtained does have a clear structure at 3.0 keV but much reduced intensity as expected.

We can see the the figures 3(D_1) and 3(F_1) display Al K_α peak (at 1.518 keV), K_α^h peak (at 1.637 keV), Ne $K_{\alpha\alpha}$ (at 1.725 keV) and Al $K_{\alpha\alpha}$ (at 3.012 KeV). These observed peaks have been compared well with the theoretical and experimental results as shown in Table I. The Table shows the K_α , K_α^h and $K_{\alpha\alpha}$ energies of Ne and Al. Al K_α , Al K_α^h and $K_{\alpha\alpha}$ transition energies are observed at 1.518 keV, 1.637 keV and 3.012 keV, respectively. While the Ne $K_{\alpha\alpha}$ transition energy is found 1.725 keV. It's an unusual observation as the Ne K_α as well as Ne K_α^h have not been observed but the Ne $K_{\alpha\alpha}$ is observed! This has happened due to the fact that much higher attenuation of K_α (≈ 0.85 keV) than the $K_{\alpha\alpha}$ (≈ 1.7 keV) as evidenced from Table III. Further, the absolute efficiency of the SDD detector for K_α is much less than that for the $K_{\alpha\alpha}$.

Making x-ray spectroscopy of light ions is very difficult, which can be understood from comparison of x-ray fluorescence yield as a function of atomic number [24, 25]. To visualise this fact we have compared the total K-level Auger transition rates (Γ_{KA} in unit of eV/ \hbar), total K x-ray emission rate (Γ_{KF} in unit of eV/ \hbar). Further, the percentage ratio of Γ_{KF} to Γ_{KA} for Ne and Al are given in Table II. We can see from the Table that value of Auger transition rate is much higher than the x-ray emission rate for K shell transitions. This ratio for Ne is only 1.89%, this for Al is 5%.

IV. SUMMARY

To the best of our knowledge such a study is made for the first time in the country. We have succeeded to get the signature of TEOP transitions for the Ne and Al system at two low energy points (90 keV/amu and 95 keV/amu). In recorded spectrum of Ne beam on Al-target, we get a prominent Bremsstrahlung background. After subtraction of the Bremsstrahlung background from the raw spectrum, we get actual spectrum. We observed TEOP transition energies for Ne at 1.725 keV and Al at 3.012 keV. We also observed Al K_α and Al K_α^h peaks at 1.518 keV, 1.637 keV energies, respectively. Within experimental uncertainty limits, these values are well matched with previously reported experimental and theoretical values. For both the projectile energies, observed values of transition energies are slightly different but within the measurement uncertainties.

V. FUTURE PLANS

We have presented significant results regarding the TEOP process, but it can only a start up. To study the TEOP process well in this laboratory, we have to upgrade our measurement system to great extent. In first instance, the beam focusing issue must be resolved. Beam need to be well focused and much smaller in size that that of the foil, in our case it is 10 mm in diameter. We saw that little higher energy will be better to have higher statistics. We can not increase the deck potential more than 350 KV, hence we have to try to increase the charge state. Hope to get Ne^{8+} for our use next time. We will put the detector closer to the target too. Further, measured production cross-section of the $K_{\alpha\alpha}$ transitions are extremely useful to test the theoretical ideads relevant to the TEOP processes. Note that x-ray production cross sections for the K x-ray lines can be determined from the following formula

$$\sigma_i^x = (Y_i^x A \text{Sin}\theta) / (N_A \epsilon n_p t \beta) \quad (1)$$

where Y_i^x is the intensity of the ith x-ray peak ($i = K_\alpha, K_\beta$), A is the atomic weight of the target, θ is the angle between the incident ion beam and the target foil normal, N_A is the Avogadro number, n_p is the number of incident projectiles, ϵ is the effective efficiency of the x-ray detector, t is the target thickness in $\mu\text{g}/\text{cm}^2$ and β is a correction factor for energy loss of the incident projectile and absorption of emitted x-rays in the target element. Nevertheless, we have not yet measured the absolute efficiency of the SDD detector. Hence, we may determine only the relative cross section of $K_{\alpha\alpha}$ with respect to K_α and K_α^h from the relative intensity ratios if we know the relative detector efficiency from any source, for example Schlosser *et al.* [27]. Though this procedure is well applicable to Al, but not so for Ne at all as we have not detected the Ne $K_{\alpha\alpha}$ and K_α^h transitions. We

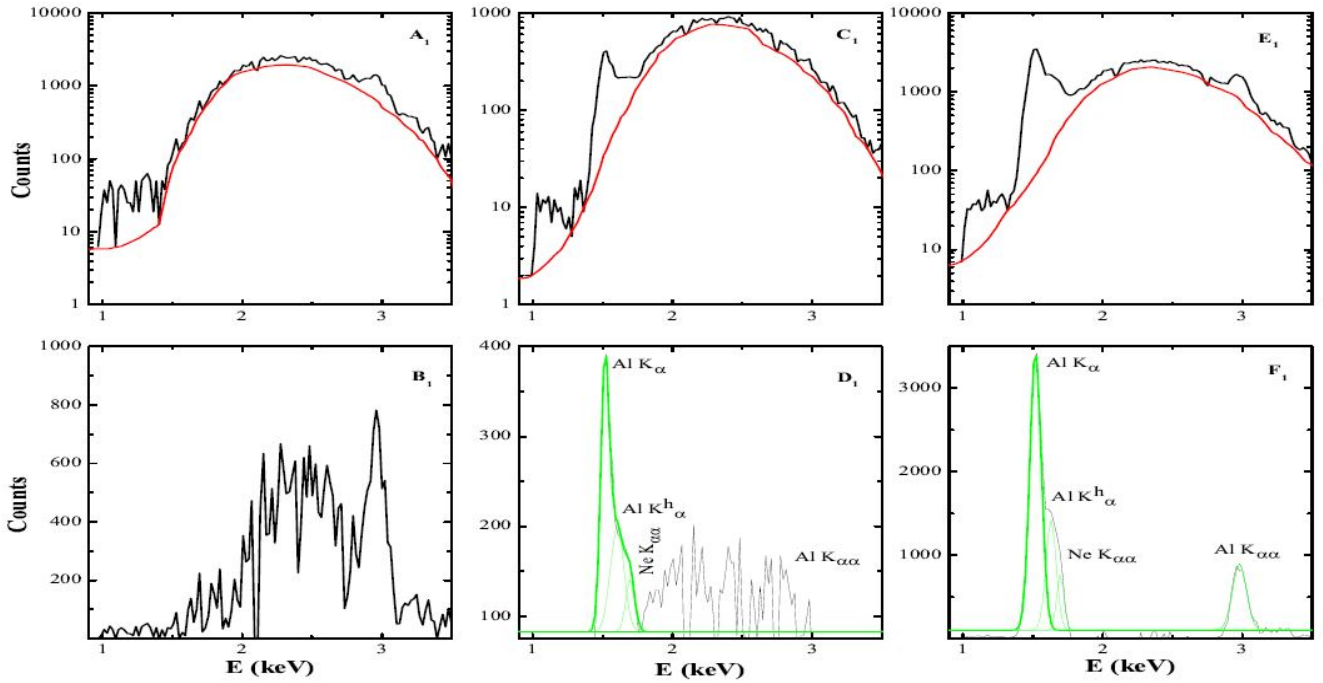


FIG. 3. (A_1) Line in black represent the spectrum of Ne on Al at 1.8 MeV energy and that in red the background spectrum, (B_1) the spectrum obtained after subtraction of the red spectrum from the black. The absolute spectrum so obtained is fitted with Gaussian peaks as shown with green curve, where E is the x-ray energy in keV and C the counts. (C_1) Line in black represent the spectrum of Ne on Al at 2.1 MeV energy and that in red the background spectrum, (D_1) the spectrum obtained after subtraction of the red spectrum from the black. The absolute spectrum so obtained is fitted with Gaussian peaks as shown with green curve, where E is the x-ray energy in keV and C the counts. (E_1) Line in black represent the raw background spectrum at 2.1 MeV energy and that in red the Bremsstrahlung background spectrum, (F_1) the spectrum obtained after subtraction of the red spectrum from the black. The absolute spectrum so obtained is shown.

TABLE I. Comparison of the transition energies (in keV) of Ne and Al K_{α} , K_{α}^h and $K_{\alpha\alpha}$ peaks observed in this experiment vs earlier theories and experiments; where, El stands for element name, for this experiment $E_1 = 1.8$ MeV and $E_2 = 2.1$ MeV, A for theoretical values reported by others, B for experimental values reported by others, ND stands for not detected in this experiment, NA - not available in literature.

El	K_{α}				K_{α}^h				$K_{\alpha\alpha}$			
	E_1	E_2	A	B	E_1	E_2	A	B	E_1	E_2	A	B
Ne	ND	ND	0.848 [21]	NA	ND	ND	NA	NA	1.707 ± 0.207	1.725 ± 0.268	1.762 [22]	1.8 [18]
Al	1.521 ± 0.237	1.518 ± 0.055	1.486 [21]	1.52 ± 0.010 [9]	1.637 ± 0.256	1.637 ± 0.117	1.622 [23]	NA	3.002 ± 0.251	3.012 ± 0.194	3.072 [17], 3.057 [23]	3.18 ± 0.020 [9], 3.056 ± 0.009 [13]

TABLE II. Auger transition rates (A_K) and x-ray emission rates (R) due to vacancy in K-shell (in unit of eV/\hbar) and percentage ratio of R to A_K for Ne and Al.

Element	A_K [26]	R [26]	R/A_K (%)
Ne	0.258	0.0049	1.89
Al	0.316	0.0158	5

TABLE III. Comparison of percentage attenuation of the intensity (%) of Ne K_{α} peak vs percentage attenuation of the intensity of Al K_{α} peak in $6\mu m$ and $10\mu m$ mylar windows

Thickness	Ne K_{α}	Al K_{α}	Ne $K_{\alpha\alpha}$	Al $K_{\alpha\alpha}$
$6\mu m$	91.33	55.11	29.76	10.25
$10\mu m$	98.30	73.68	44.50	16.50

can think of two remedies for this issue. Number one is to place the SDD detector inside the vacuum chamber and number two is to measure the quantum efficiency of the detector. It appears the first option is too difficult to adapt for the SDD detector of our disposal. Hence, we plan to measure the over all detector efficiency (including solid angle, mylar window and air gap between

the detector and mylar window etc.) by using the proton beam of 350 keV and the targets possibly from Mg to Ge.

It is well known that for the light elements, rate of Auger transition is much higher than fluorescence rate. So we will add an experimental set up for electron spectroscopy in this experiment in future which will give us

TABLE IV. Production cross-sections (σ^{xK_α} , $\sigma^{xK_\alpha^h}$, $\sigma^{xK_{\alpha\alpha}}$ (in unit of mili-barn)) of the transitions Al K_α , Al K_α^h , Ne $K_{\alpha\alpha}$ and Al $K_{\alpha\alpha}$; the ratio of Al K_α^h , Ne $K_{\alpha\alpha}$ and Al $K_{\alpha\alpha}$ to the Al K_α

E (MeV)	$\sigma^{xK_\alpha}(Al)$	$\sigma^{xK_\alpha^h}(Al)$	$\sigma^{xK_{\alpha\alpha}}(Ne)$	$\sigma^{xK_{\alpha\alpha}}(Al)$	$\frac{\sigma^{xK_\alpha^h}(Al)}{\sigma^{xK_\alpha}(Al)}$	$\frac{\sigma^{xK_{\alpha\alpha}}(Ne)}{\sigma^{xK_\alpha}(Al)}$	$\frac{\sigma^{xK_{\alpha\alpha}}(Al)}{\sigma^{xK_\alpha}(Al)}$
1.8	122	20	10	0.8	0.164	0.082	0.00656
2.1	694	82	25	3.6	0.118	0.036	0.00519

TABLE V. The value of absolute intensity (I: in the multiple of 10^6) of the transitions K_α , K_α^h , $K_{\alpha\alpha}$; intensity ratios of K_α^h , $K_{\alpha\alpha}$ transitions to K_α transition

E (MeV)	$I_{K_\alpha}(Al)$	$I_{K_\alpha^h}(Al)$	$I_{K_{\alpha\alpha}}(Ne)$	$I_{K_{\alpha\alpha}}(Al)$	$\frac{I_{K_\alpha^h}(Al)}{I_{K_\alpha}(Al)}$	$\frac{I_{K_{\alpha\alpha}}(Ne)}{I_{K_\alpha}(Al)}$	$\frac{I_{K_{\alpha\alpha}}(Al)}{I_{K_\alpha}(Al)}$
1.8	203	33.2	16.8	1.45	0.164	0.083	0.007
2.1	2420	285	85.7	12.6	0.118	0.035	0.005

higher statistics and thus can understand better the two electron and one photon phenomenon. Note that the electron spectroscopy has not yet been applied for the study of two electron and one photon processes.

ACKNOWLEDGMENTS

One of the authors, Shashank Singh is thankful to the staff of LEIBF facility of IUAC (New Delhi, India) for providing excellent beam and necessary facilities for the experiment.

-
- [1] W. Heisenberg, Zur quantentheorie der multiplettstruktur und der anomalen zeemaneffekte, in *Original Scientific Papers Wissenschaftliche Originalarbeiten* (Springer, 1985) pp. 306–325.
- [2] E. Condon, The theory of complex spectra, *Physical Review* **36**, 1121 (1930).
- [3] S. Goudsmit and L. Gropper, Many-electron selection rules, *Physical Review* **38**, 225 (1931).
- [4] W. Wölfl, C. Stoller, G. Bonani, M. Suter, and M. Stöckli, Two-electron-one-photon transitions in heavy-ion collisions, *Physical Review Letters* **35**, 656 (1975).
- [5] T. Åberg, K. Jamison, and P. Richard, Origin of two-electron, one-photon k—x-ray transitions, *Physical Review Letters* **37**, 63 (1976).
- [6] W. Wölfl and H. D. Betz, Calculation of two-electron, one-photon k—x-ray transition energies, *Physical Review Letters* **37**, 61 (1976).
- [7] D. Nagel, P. Burkhalter, A. Knudson, and K. Hill, Two-electron, one-photon k x-ray transition energies, *Physical Review Letters* **36**, 164 (1976).
- [8] A. Knudson, K. Hill, P. Burkhalter, and D. Nagel, Energies and relative intensities of $k\alpha\alpha$ x-ray transitions, *Physical Review Letters* **37**, 679 (1976).
- [9] C. Stoller, W. Wölfl, G. Bonani, M. Stöckli, and M. Suter, Two-electron one-photon transitions into the doubly ionized k shell, *Physical Review A* **15**, 990 (1977).
- [10] J. Auerhammer, H. Genz, A. Kumar, and A. Richter, Two-electron-one-photon transition in aluminum following double-k-shell ionization, *Physical Review A* **38**, 688 (1988).
- [11] T. K. Mukherjee, J. Ghosh, and S. Sengupta, Branching ratio of two-electron—one-photon transitions in doubly ionized low-z atoms, *Physical Review A* **42**, 3125 (1990).
- [12] T. Mukherjee and P. Mukherjee, Two electron one photon transitions in atomic systems, *Zeitschrift für Physik D Atoms, Molecules and Clusters* **42**, 29 (1997).
- [13] J. Hoszowska, J.-C. Dousse, J. Szlachetko, Y. Kayser, W. Cao, P. Jagodziński, M. Kavčič, and S. Nowak, First observation of two-electron one-photon transitions in single-photon k-shell double ionization, *Physical review letters* **107**, 053001 (2011).
- [14] S. Kasthurirangan, J. Saha, A. Agnihotri, S. Bhat-tacharyya, D. Misra, A. Kumar, P. Mukherjee, J. Santos, A. Costa, P. Indelicato, *et al.*, Observation of $2p3d(1p\ o)\rightarrow 1s3d(1d\ e)$ radiative transition in he-like si, s, and cl ions, *Physical review letters* **111**, 243201 (2013).
- [15] R. Diamant, S. Huotari, K. Hämäläinen, C. Kao, and M. Deutsch, Cu k h α 1, 2 hypersatellites: Suprathreshold evolution of a hollow-atom x-ray spectrum, *Physical Review A* **62**, 052519 (2000).
- [16] J. Briand, Two-electron, one-photon transition energies, *Physical Review Letters* **37**, 59 (1976).
- [17] R. Kadrekar and L. Natarajan, Two-electron one-photon transitions in atoms with $12\leq z\leq 80$, *Journal of Physics B: Atomic, Molecular and Optical Physics* **43**, 155001 (2010).
- [18] S. Andriamonje, H. Andrä, and A. Simionovici, Two electron-one photon x-ray emission in slow collisions between fully stripped ions and solids, *Zeitschrift für Physik D Atoms, Molecules and Clusters* **21**, S349 (1991).
- [19] T. Mukherjee, T. Ghosh, and P. Mukherjee, On the interpretation of two electron-one photon transitions in slow collisions between fully stripped ions and solid target, *Zeitschrift für Physik D Atoms, Molecules and Clusters* **33**, 7 (1995).
- [20] D. FREEDOM, acquisition and analysis software, designed to support accelerator based experiments at the iuac, New Delhi, India.
- [21] H. Winick, X-ray data booklet, X-RAY DATA BOOKLET (2009).
- [22] M. Gavrilin and J. Hansen, Calculation of $k\alpha\alpha$ and $k\alpha\alpha^h$

- transition rates, *Physics Letters A* **58**, 158 (1976).
- [23] J. Saha, T. Mukherjee, S. Fritzsche, and P. Mukherjee, The effect of a 2s vacancy on two-electron–one-photon lines: Relativistic approach, *Physics Letters A* **373**, 252 (2009).
- [24] M. H. Chen, B. Crasemann, and H. Mark, Relativistic k-shell auger rates, level widths, and fluorescence yields, *Physical Review A* **21**, 436 (1980).
- [25] M. H. Chen, Auger transition rates and fluorescence yields for the double-k-hole state, *Physical Review A* **44**, 239 (1991).
- [26] E. McGuire, K-shell auger transition rates and fluorescence yields for elements ar-xe, *Physical Review A* **2**, 273 (1970).
- [27] D. Schlosser, P. Lechner, G. Lutz, A. Niculae, H. Soltau, L. Strüder, R. Eckhardt, K. Hermenau, G. Schaller, F. Schopper, *et al.*, Expanding the detection efficiency of silicon drift detectors, *Nuclear Instruments and Methods in Physics Research Section A: Accelerators, Spectrometers, Detectors and Associated Equipment* **624**, 270 (2010).
- [28] L. Natarajan, Single-photon emission from simultaneous two-electron transitions in he-like ions, *Physical Review A* **90**, 032509 (2014).
- [29] J. Rzadkiewicz, D. Chmielewska, T. Ludziejewski, P. Rymuza, Z. Sujkowski, D. Castella, D. Corminboeuf, J.-C. Dousse, B. Galley, C. Herren, *et al.*, He-like hole states in mid-z atoms studied by high-resolution k x-ray spectroscopy, *Physics Letters A* **264**, 186 (1999).
- [30] W. Bambynek, B. Crasemann, R. Fink, H.-U. Freund, H. Mark, C. Swift, R. Price, and P. V. Rao, X-ray fluorescence yields, auger, and coster-kronig transition probabilities, *Reviews of modern physics* **44**, 716 (1972).
- [31] V. O. Kostroun, M. H. Chen, and B. Crasemann, Atomic radiation transition probabilities to the 1 s state and theoretical k-shell fluorescence yields, *Physical Review A* **3**, 533 (1971).
- [32] J. H. Scofield, Radiative decay rates of vacancies in the k and l shells, *Physical Review* **179**, 9 (1969).
- [33] J. H. Hubbell and S. M. Seltzer, *Tables of X-ray mass attenuation coefficients and mass energy-absorption coefficients 1 keV to 20 MeV for elements Z= 1 to 92 and 48 additional substances of dosimetric interest*, Tech. Rep. (National Inst. of Standards and Technology-PL, Gaithersburg, MD (United . . . , 1995).